Technical Note

Comparison of numerical and experimental drag measurement in hypervelocity flow

A. L. SMITH, I. A. JOHNSTON and K. J. AUSTIN
Department of Mechanical Engineering
The University of Queensland, St Lucia, Queensland, Australia

1. INTRODUCTION

In planning interplanetary missions which involve an aerobraking manoeuvre, it is necessary to make accurate predictions of the aerodynamic drag acting on a vehicle during its descent. Of interest to the authors is the Nasa initiative for exploration of Mars and its atmosphere. The Mars Pathfinder[1] is a probe that is expected to enter the Martian atmosphere at a relative velocity of approximately 7·6 kms^{-1}. The forebody of this vehicle is based on a 70° blunted cone and is typical of aerobraking designs.

In this note, a comparison is made between experimental and numerical techniques for predicting drag in hypervelocity flow. Three different models were examined in this study: a 30° sharp cone; an Apollo[2] heat shield; and a Viking[3] heat shield. A relatively simple analytical result for the drag on a cone provides a convenient reference for both the experimental and numerical results. The two heat shields are typical of those used for interplanetary exploration, such as the Mars Pathfinder. Our aim is to give an example of how computational fluid dynamics can be used in conjunction with experiments to obtain information about the hypervelocity flow about re-entry vehicles.

Experimental drag results for the three models were obtained using a stress wave force balance[4]. The experiments were conducted in a test flow of partially dissociated carbon dioxide, generated using a free-piston driven expansion tube. For comparison, two different numerical techniques were used. The first, a Navier-Stokes code, allowed the effects of chemistry and viscosity to be investigated and their relative influence on experimental results determined. A second numerical code based on Newtonian flow theory was also used. This code provided rapid analysis enabling the sensitivity of experimental results to angular misalignment of the model and variations in test flow conditions to be determined.

2. EXPERIMENTAL TECHNIQUE

The experimental technique presented here has been used to measure axial drag[5] on short models in both shock tube and expansion tube facilities. Details of the technique are discussed in Ref. 4, with only a brief description given here.

Manuscript received 29 April 1996, revised version received 16 August 1996, accepted 23 September 1996.
Paper No. 2194.

The experiments were conducted in the X1 facility located at The University of Queensland. The facility was operated as an expansion tube producing approximately 50 μs of steady test flow at a velocity of 7·5 kms^{-1}. This corresponds to at least 27 body lengths of test flow for all of the models used. Carbon dioxide was used as the test gas, with the test flow conditions being determined by assuming equilibrium chemistry[6]. These test conditions are presented in Table 1, along with the respective uncertainties. The characteristically short test times of this facility prohibit the use of traditional force measurement techniques. To overcome this limitation a stress wave force balance[4] was used. A schematic representation of the stress wave force balance and the models tested are presented in Fig. 1.

The stress wave force balance involves connecting the model to an elastic stress bar and suspending the arrangement in the test flow so that there is no restriction to movement in the flow direction. Stress waves produced by the sudden arrival of the test flow are reflected within the stress bar and are measured using strain gauges. The dynamic behaviour of the arrangement can be modelled as a linear system in which the input is the drag force on the model, and the output is the measured strain time history. An impulse response function is then used to describe the relationship between the input and output. In experiments, the unknown drag force on the model is determined from the measured strain time history and the impulse response function. Thus the problem is an inverse one and the drag may be found using a numerical deconvolution procedure.

Table 1
Test flow conditions used for experimental and numerical tests
† Reynolds number based on maximum model diameter

Test conditions		Uncertainty
Flow velocity (ms^{-1})	7500	±2·0%
Static pressure (kPa)	15·6	±2·0%
Pitot pressure (kPa)	1230	±2·0%
Temperature (K)	2990	±1·9%
Density (kgm^{-3})	0·0194	±10·0%
Stagnation enthalpy (MJkg^{-1})	36·8	±2·6%
Specific heat ratio	1·25	±5·0%
Freestream Reynolds number† (cone)	2·9×10^5	±10·4%
Freestream Reynolds number† (heat shields)	3·6×10^5	±10·4%
Mach number	7·4	±4·3%
Flow composition (mass fraction)		
Molecular oxygen (O_2)	0·189	
Atomic oxygen (O)	0·062	
Carbon dioxide (CO_2)	0·310	
Carbon monoxide (CO)	0·439	
Atomic carbon (C)	0·000	

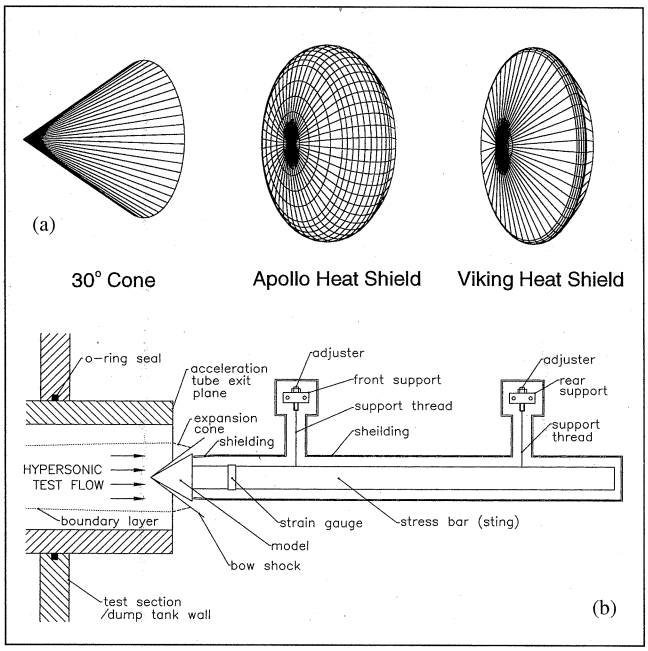

Figure 1. (a) The cone, Apollo and Viking model geometries, and (b) a schematic of the stress wave force balance.

3. NUMERICAL TECHNIQUES

A time-accurate finite volume Navier-Stokes integrator[7] was used to calculate flowfields over a structured computational domain. The forebody flowfield was found for all test cases, with the inclusion of the expansion region around the shoulders of the heat shield models. Second order temporal and spatial accuracy was achieved with Runge-Kutta time stepping and *MUSCL* interpolation respectively. The use of shock fitting over the blunt bodies enhanced solution stability, and avoided the occurrence of problems such as the carbuncle effect[8], and those reported in Ref. 9. Shock fitting also improved computational efficiency since, unlike shock capturing, the steady inflow upstream of the bow shock wave does not occupy part of the solution domain. Mass, momentum and energy fluxes between cells were found by an approximate Riemann solver for the shock captured cone, while the advection upwind splitting method[10] (AUSM) was used for the shock fitted blunt bodies. Where AUSM was used, some filtering of results was applied to remove noise inherent to the scheme. Chemistry and viscosity were simulated with a simple five species, three reaction equilibrium carbon dioxide model[11]. Simulations with the gas chemistry frozen at inflow conditions were also performed with this code.

Solutions were marched in time until the flow had passed the body by a length of at least 25 body diameters. This allowed variations in drag to settle to acceptably small levels. Grid independence of the solution was checked by doubling the mesh resolution (from 2250 to 9000 finite volume cells) for the Apollo case. The difference between the results was less than 0·07%. The typical CPU time for a viscous heat shield solution on a Silicon Graphics Power Challenge Array was 18 hours on a single processor.

In contrast to the finite volume code, the Newtonian solver[12] enabled calculation of aerodynamic forces in a few seconds on a small workstation. Newtonian theory is a local surface inclination method, neglecting high temperature, viscous and boundary layer effects. Methods applying this principle have been well used on a range of geometries in hypervelocity flow, particularly where the pressure distribution is dominated by pressure drag rather than viscous effects[13]. For a body surface defined as a collection (mesh) of locally flat surface elements, Newtonian theory is applied independently to these elements to provide a complete surface pressure distribution. By modifying the standard Newtonian sine-squared law, the pressure coefficient at the stagnation point is made to agree with normal shock wave theory. This provides more accurate pressure distributions over blunt bodies[14], and introduces a Mach number dependency. Since free stream particles can only impact the frontal area in the Newtonian model, regions shadowed by the incident flow are assumed to have a surface pressure equivalent to the freestream. For each of the predictions the surface mesh was refined so that differences in the drag between successive refinements were less than 1%. In general the Newtonian technique becomes inaccurate when the shock shape and body shape are not well aligned.

4. RESULTS AND DISCUSSION

The results are divided into two parts. The first part is a comparison between the experimental and numerical results and an accepted analytical solution[15] for the drag force on a 30° cone. The second part involves a comparison between the experimental and numerical results for two typical re-entry type vehicle configurations. The carbon dioxide test flow conditions for each case are the same, and appear in Table 1.

The uncertainty in drag associated with the experimental technique was ±10% for each test. This uncertainty is primarily due to the high sensitivity of the freestream conditions to the measured shock speed, known only to ±2%. The tabulated experimental drag coefficients have been averaged over at least two tests.

For all three cases, the effect of pressure on the model base region was minimised through use of flow shielding on the experimental rig. An estimate of this pressure was made by assuming that the pressure in the base region starts at the initial test section pressure (approximately 100 Pa), and rises with time as gas leaks through the gap between the shielding and the model (Fig. 1(b)). This build up of pressure is calculated by assuming choked flow from the conditions behind the shock on the model. The results from these calculations indicated that the effect of pressure in the base region was negligible. Correspondingly, the contribution of this pressure to base drag was neglected in both numerical simulations.

4.1 Cone model

An analytical solution for drag on the 30° cone (of base diameter 16 mm) was generated by the Taylor-Macoll method[15], assuming inviscid flow of an ideal gas with frozen chemistry. Using this result, the Navier-Stokes code was verified by running under the same flow assumptions. The two calculated drag values agreed to within 0·1%. The code was then used to predict the drag for a viscous flow in chemical equilibrium. The results in Table 2 show excellent agreement between experiment and Navier-Stokes calculation. The effect of chemistry on the total drag was found to be negligible. The viscous contribution to drag was more significant, being 4·7%. The Newtonian solver gave a drag coefficient differing 12% from experiment, thus lying outside the experimental uncertainty band. This discrepancy can in part be attributed to the contribution of viscous forces on the model. The remainder of the difference arises from the assumptions inherent to the Newtonian solver not being satisfied for this test case.

4.2 Heat shield models

Prediction of drag for the heat shields (each with a maximum diameter of 20 mm) using both numerical techniques agreed with

Model	Drag coefficient of model				
	Experimental	Newtonian	Navier-Stokes†‡ Equilibrium	Navier-Stokes†‡ Frozen	T-M*
30° cone	0·57±10%	0·50	0·57±0·3%	0·57±0·3%	0·54
Apollo heat shield	1·54±10%	1·50	1·41±0·5%	1·42±0·8%	–
Viking heat shield	1·78±10%	1·62	1·68±0·5%	1·71±0·5%	–

Table 2
Summary of results

† Quantity includes viscous contribution to drag.
‡ Error bands indicate time transient variation in drag.
* Taylor-Macoll method only applicable to inviscid cone solutions.

experiment to within the uncertainty range. However, the computed estimates were consistently below the experimental values.

Equilibrium chemistry had a small influence on heat shield drag computed using the Navier-Stokes code. Equilibrium chemistry increased drag by approximately 1% for the Apollo and 2% for the Viking heat shield. The contribution of viscous forces to the drag was also small, being close to 0·5% in each case.

It should be noted that the similarity of results from frozen and equilibrium chemistry simulations does not necessarily indicate that chemistry considerations are unimportant. It is possible that the non-equilibrium drag force may lie outside the bounds of that calculated from frozen and equilibrium simulation results. Macrossan[16] has shown that for a blunt body in a reacting hypervelocity flow the non-equilibrium surface pressure distribution differs from that of frozen and equilibrium flow, an effect which is attributed to quenching[17]. The quenching process is characterised by a region of intense reaction close to the shock, where the temperature falls rapidly. Consequently the dissociation reaction rate falls exponentially, producing a large region of chemically frozen flow that expands around the blunt body. Thus quenching may affect the distribution of surface pressure on the body, and hence alter the experimental drag.

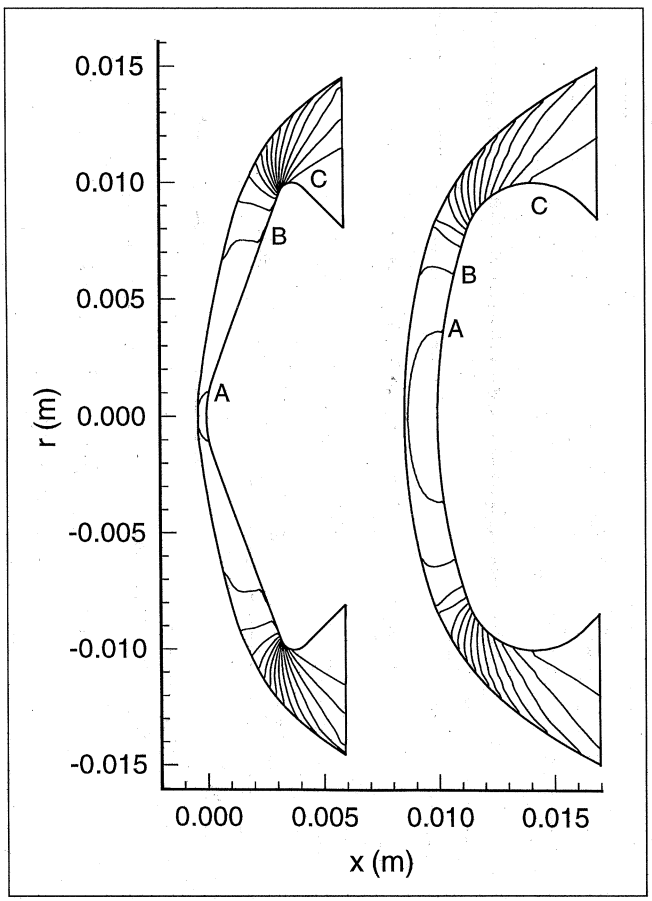

Figure 2. Isopressure contours around the Viking and Apollo heat shields, determined using the Navier-Stokes code. Labelled contour levels are A, 1·035 MPa; B, 0·966 MPa; and C, 0·072 MPa.

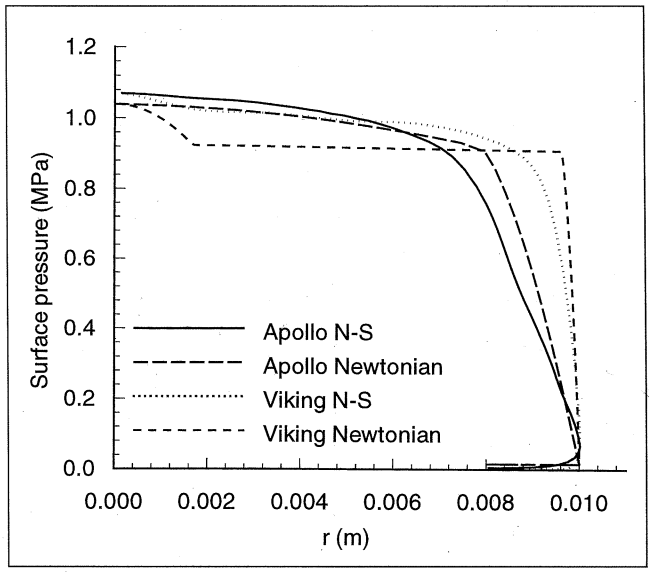

Figure 3. Surface pressure profiles for the Apollo and Viking heat shields, determined using the Newtonian solver and Navier-Stokes code.

The Apollo and Viking heat shield pressure fields generated by the Navier-Stokes code are shown in Fig. 2. For the Apollo heat shield, the shock shape is observed to match the body shape closely, until expansion around the model edge occurs. This satisfies the Newtonian solver assumptions, and thus close agreement with the Navier-Stokes code is achieved for this case. For the Viking heat shield there was an observable difference between the shock and body shapes, and the Newtonian solver did not perform as well. The drag coefficients calculated by the Newtonian solver agreed to within experimental uncertainty for both heat shields, and produced solutions typically five orders of magnitude faster than the Navier-Stokes code. The radial surface pressure profiles for the heat shields were produced using both codes, and are compared in Fig. 3.

Having verified the accuracy of the Newtonian solver, Newtonian theory was used to predict the effect of variations in the test flow conditions. As expected with a Newtonian analysis, the drag varied directly with the density and the square of velocity. The sensitivity of drag to angular misalignment was also investigated over a range of pitch angles from 0° to 15°. Over this small range the heat shield drag varied approximately with the square of the incident angle, decreasing to a difference of less than 1% at 5°. The angular misalignment present during experiments is estimated at less than 1° which would correspond to a difference of less than 0·2% in the true and measured drag.

5. CONCLUSION

This study demonstrates the capability to predict and measure drag forces in hypersonic flow of carbon dioxide. Two numerical techniques were used to illustrate the relative importance of factors affecting the drag estimate. Using a Navier-Stokes code, it was found that viscous and equilibrium chemistry effects did not

significantly alter drag results. Additionally, agreement between the code and experimental results for drag of a 30° cone was excellent. The Newtonian technique proved to be a useful tool in obtaining drag predictions rapidly with reasonable accuracy. The calculated drag on two typical re-entry type heat shields was found to lie within experimental uncertainty.

ACKNOWLEDGEMENTS

Experimental work was conducted under Australian Research Council grant A8941305. Computer simulations were run at the University of Queensland High Performance Computing Facility. The authors are grateful for the assistance of P.A. Jacobs and D.J. Mee.

REFERENCES

1. CHEN, Y.K., HENLINE, W.D. and TAUBER, M.E. Mars Pathfinder trajectory base heating and ablation calculation, *J Spacecr Rock*, 1995, **32**, (2), pp 225-230.
2. PARK, C. *Nonequilibrium Hypersonic Aerothermodynamics*, John Wiley and Sons, New York, 1990.
3. MILLER, C.G. Shock shapes on blunt bodies in hypersonic-hypervelocity helium, air and CO_2 flows, and calibration results in Langely 6-inch expansion tube, NASA TN D-7800, 1975.
4. SMITH, A.L. and MEE, D.J. Drag measurements in a hypervelocity expansion tube, *Int J Shock Waves*, 1996 (accepted).
5. TUTTLE, S.L., MEE, D.J. and Simmons, J.M. Drag measurement at Mach 5 using a stress wave force balance, *Exp in Fluids*, 1995, **19**, pp 336-341.
6. NEELY, A.J. and MORGAN, R.G. The Superorbital Expansion Tube concept, experiment, and analysis, *Aeronaut J*, March 1994, **98**, (973), pp 97-105.
7. JOHNSTON, I.A. and JACOBS, P.A. SF2D: A Shock Fitting and Capturing Solver for Two Dimensional Compressible Flows, Dept of Mechanical Engineering, University of Queensland, Technical Report No 6/96, 1996.
8. QUIRK, J.J. A contribution to the great Riemann solver debate, *Int J Numer Methods in Fluids*, 1994, **18**, (6), pp 555-574.
9. JOHNSTON, I.A. and JACOBS, P.A. Hypersonic blunt body flows in reacting carbon dioxide, Twelfth Australasian Fluid Mechanics Conference, 1995, **2**, pp 807-810.
10. LIOU, M.-S. and STEFFEN, C.J. A New flux splitting scheme, *J Comp Phys*, 1993, **107**, pp 23-39.
11. JOHNSTON, I.A., A Thermodynamic Model of the Martian Atmosphere for Computational Fluid Dynamics Analyses, Dept of Mechanical Engineering, University of Queensland, Honours Thesis, 1994.
12. AUSTIN, K.J. and JACOBS, P.A. A Newtonian Solver for Hypersonic Flows, Dept of Mechanical Engineering, University of Queensland, Technical Report, No 5/96, 1996.
13. MAUGHMER, M., OZOROSKI, L., STRAUSSFOGEL, D. and LONG L. Validation of engineering methods for predicting hypersonic vehicle control forces and moments, *J Guid Contr Dynam*, 1993, **16**, (4).
14. ANDERSON, J.D. *Hypersonic and High Temperature Gas Dynamics*, McGraw-Hill, 1989.
15. TAYLOR, G.I. and MACCOLL, J.W. The Air Pressure on a Cone Moving at High Speed, Proc Royal Society (London) Series A: Mathematical and Physical Sciences, **139**, (A8383), 1932, pp 278-311.
16. MACROSSAN, M.N. Hypervelocity flow of dissociating nitrogen downstream of a blunt nose, *J Fluid Mech*, 1990, **217**, 1990, pp 167-202.
17. STALKER, R.J. Approximations for non-equilibrium hypervelocity aerodynamics, Annual Review Fluid Mechanics, 1989, **21**, pp 37-60.